LETTER

The intense starburst HDF 850.1 in a galaxy overdensity at $z \approx 5.2$ in the Hubble Deep Field

Fabian Walter[1,2], Roberto Decarli[1], Chris Carilli[2,3], Frank Bertoldi[4], Pierre Cox[5], Elisabete Da Cunha[1], Emanuele Daddi[6], Mark Dickinson[7], Dennis Downes[5], David Elbaz[6], Richard Ellis[8], Jacqueline Hodge[1], Roberto Neri[5], Dominik A. Riechers[8], Axel Weiss[9], Eric Bell[10], Helmut Dannerbauer[11], Melanie Krips[5], Mark Krumholz[12], Lindley Lentati[3], Roberto Maiolino[3,13], Karl Menten[9], Hans-Walter Rix[1], Brant Robertson[14], Hyron Spinrad[15], Dan P. Stark[14] & Daniel Stern[16]

The Hubble Deep Field provides one of the deepest multiwavelength views of the distant Universe and has led to the detection of thousands of galaxies seen throughout cosmic time[1]. An early map of the Hubble Deep Field at a wavelength of 850 micrometres, which is sensitive to dust emission powered by star formation, revealed the brightest source in the field, dubbed HDF 850.1 (ref. 2). For more than a decade, and despite significant efforts, no counterpart was found at shorter wavelengths, and it was not possible to determine its redshift, size or mass[3–7]. Here we report a redshift of $z = 5.183$ for HDF 850.1, from a millimetre-wave molecular line scan. This places HDF 850.1 in a galaxy overdensity at $z \approx 5.2$, corresponding to a cosmic age of only 1.1 billion years after the Big Bang. This redshift is significantly higher than earlier estimates[3,4,6,8] and higher than those of most of the hundreds of submillimetre-bright galaxies identified so far. The source has a star-formation rate of 850 solar masses per year and is spatially resolved on scales of 5 kilopsecs, with an implied dynamical mass of about 1.3×10^{11} solar masses, a significant fraction of which is present in the form of molecular gas. Despite our accurate determination of redshift and position, a counterpart emitting starlight remains elusive.

We have obtained a full-frequency scan of the 3-mm band towards the Hubble Deep Field using the IRAM (Institut de Radioastronomie Millimétrique) Plateau de Bure Interferometer. The observations covered the frequency range from 80–115 GHz in ten frequency settings at uniform sensitivity and at a resolution (about 2.3′′) that is a good match to galaxy sizes at high redshift. They resulted in the detection of two lines of carbon monoxide (CO), the most common tracer for molecular gas at high redshift[9], at 93.20 GHz and 111.84 GHz at the position of HDF 850.1. Identifying these lines with the $J = 5$ and $J = 6$ rotational transitions of CO gives a redshift for HDF 850.1 of $z = 5.183$. This redshift was then unambiguously confirmed by the Plateau de Bure Interferometer's detection of the 158-μm line of ionized carbon ([C II], redshifted to 307.38 GHz), one of the main cooling lines of the star-forming interstellar medium. Stacking of other molecules covered by our frequency scan that trace higher volume densities did not lead to a detection (see Supplementary Information). Subsequently, the $J = 2$ line of CO has also been detected using the National Radio Astronomy Observatory (NRAO) Jansky Very Large Array at 37.29 GHz. The observed [C II] and CO spectra towards HDF 850.1 are shown in Fig. 1.

The beam size of our CO observations (about 2.3′′, 15 kpc at $z = 5.183$) is too large to spatially resolve the molecular gas emission in HDF 850.1. However, the [C II] and underlying continuum

observations (around $1.2'' \times 0.8''$) show that the source is extended (hitherto, the interstellar medium has been spatially resolved only in
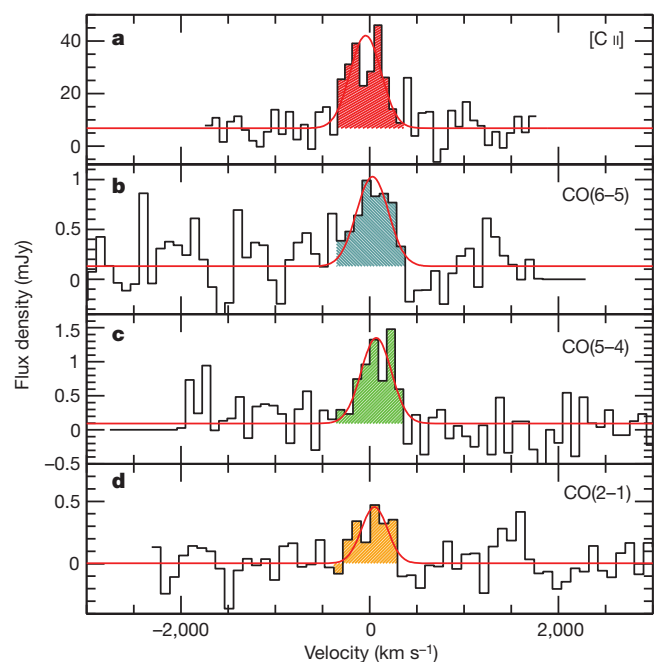

Figure 1 | Detection of four lines tracing the star-forming interstellar medium in HDF 850.1. a, [C II], $\nu_{obs} = 307.383$ GHz. **b**, CO(6–5), $\nu_{obs} = 111.835$ GHz. **c**, CO(5–4), $\nu_{obs} = 93.202$ GHz. **d**, CO(2–1), $\nu_{obs} = 37.286$ GHz. Zero velocity corresponds to a redshift of $z = 5.183$. Continuum emission is detected in **a** and **b** at 6.80 ± 0.8 mJy and 0.13 ± 0.03 mJy, respectively. We derive a 3σ continuum limit of 30 μJy from the Jansky Very Large Array observations at 37.3 GHz using a bandwidth larger than shown here. Gaussian fits to the lines give a full width at half maximum (FWHM) of 400 ± 30 km s^{-1}, narrower than typically found in sub-millimetre selected galaxies[13]. The observed integrated line flux densities are: $S_{[C II]} = 14.6 \pm 0.3$ Jy km s^{-1}, $S_{[CO(6–5)]} = 0.39 \pm 0.1$ Jy km s^{-1}, $S_{[CO(5–4)]} = 0.50 \pm 0.1$ Jy km s^{-1} and $S_{[CO(2–1)]} = 0.17 \pm 0.04$ Jy km s^{-1}. The resulting line luminosities are[9] 5.0×10^{10} K km s^{-1} pc^2, 1.0×10^{10} K km s^{-1} pc^2, 1.9×10^{10} K km s^{-1} pc^2 and 4.1×10^{10} K km s^{-1} pc^2 or $1.10 \times 10^{10} L_{Sun}$, $1.06 \times 10^{8} L_{Sun}$, $1.14 \times 10^{8} L_{Sun}$ and $1.5 \times 10^{7} L_{Sun}$ (uncertainties as given for integrated line flux densities). Large velocity gradient modelling gives a predicted CO(1–0) line luminosity of 4.3×10^{10} K km s^{-1} pc^2.

[1]Max-Planck Institut für Astronomie, Königstuhl 17, D-69117, Heidelberg, Germany. [2]National Radio Astronomy Observatory, Pete V. Domenici Array Science Center, PO Box O, Socorro, New Mexico 87801, USA. [3]Cavendish Laboratory, University of Cambridge, 19 J J Thomson Avenue, Cambridge CB3 0HE, UK. [4]Argelander Institute for Astronomy, University of Bonn, Auf dem Hügel 71, 53121 Bonn, Germany. [5]IRAM, 300 rue de la Piscine, F-38406 Saint-Martin d'Hères, France. [6]Laboratoire AIM, CEA/DSM-CNRS-Université Paris Diderot, Irfu/Service d'Astrophysique, CEA Saclay, Orme des Merisiers, 91191 Gif-sur-Yvette cedex, France. [7]National Optical Astronomy Observatory, 950 North Cherry Avenue, Tucson, Arizona 85719, USA. [8]Astronomy Department, California Institute of Technology, MC105-24, Pasadena, California 91125, USA. [9]Max-Planck-Institut für Radioastronomie, Auf dem Hügel 69, 53121 Bonn, Germany. [10]Department of Astronomy, University of Michigan, 500 Church Street, Ann Arbor, Michigan 48109, USA. [11]Universität Wien, Institut für Astronomie, Türkenschanzstraße 17, 1080 Wien, Austria. [12]Department of Astronomy and Astrophysics, University of California, Santa Cruz, California 95064, USA. [13]INAF-Osservatorio Astronomico di Roma, via di Frascati 33, 00040 Monte Porzio Catone, Italy. [14]Department of Astronomy, University of Arizona, 933 North Cherry Avenue, Tucson, Arizona 85721, USA. [15]Department of Astronomy, University of California at Berkeley, Berkeley, California 94720, USA. [16]Jet Propulsion Laboratory, California Institute of Technology, 4800 Oak Grove Drive, Pasadena, California 91109, USA.

extremely rare quasar host galaxies at such high redshifts[10]). A single Gaussian fit yields a deconvolved size of $0.9 \pm 0.3''$, or 5.7 ± 1.9 kpc, at the redshift of the source. Figure 2 shows the maps of total [C II] emission (Fig. 2a) as well as the red- and blue-shifted parts of the [C II] line (Fig. 2b) superposed on the deepest available Hubble Space Telescope images of the Hubble Deep Field[1]. The derived dynamical mass is $M_{dyn} \approx 1.3 \pm 0.4 \times 10^{11} M_{Sun}$, assuming an arbitrary inclination of $30°$. An alternative interpretation is that the source is a merger of two galaxies, rather than a single rotating disk, which would lower the implied dynamical mass. Figure 2 shows that the source is completely obscured in the observed optical and near-infrared wavebands (that is, the rest-frame ultraviolet). There is no indication of HDF 850.1 harbouring an active galactic nucleus powered by a supermassive black hole (quasar)[11].

The CO(6–5)/CO(2–1) line luminosity ratio (in units of K km s^{-1} pc^2) (ref. 9) is 0.23 ± 0.05. Assuming that the gas is being emitted from the same volume, this implies that the high-J CO emission is sub-thermally excited on galactic scales, less than seen in the nuclei of local starburst galaxies[12]. Using a standard large velocity gradient model we find that the observed CO line intensities can be fitted with a moderate molecular hydrogen density of $10^{3.2}$ cm^{-3} and a kinetic temperature of 45 K for virialized clouds (velocity gradient $dv/dr = 1.2$ km s^{-1} pc^{-1}). We caution that these numbers would change if the CO transitions were not emitted from the same volume. The predicted CO(1–0) line luminosity is 4.3×10^{10} K km s^{-1} pc^2, close to the measured value for CO(2-1). Depending on the choice of α, the CO-to-H$_2$ conversion factor, this line luminosity implies a molecular gas mass of $M_{H2} = 3.5 \times (\alpha/0.8) \times 10^{10} M_{Sun}$; here $\alpha = 0.8$, in units of M_{sun} (K km s^{-1} pc^2)$^{-1}$, is the conversion factor adopted for ultraluminous infrared galaxies (ULIRGs)[13] and thought to be applicable to sub-millimetre bright objects[14]. The implied molecular gas mass fraction is $M_{H2}/M_{dyn} \sim 0.25 \pm 0.08$ ($\alpha/0.8$); that is, even with a low ULIRG conversion factor the molecular gas constitutes a significant fraction of the overall dynamical mass. This molecular gas mass (and fraction) is comparable to what is found in other sub-millimetre bright galaxies that are typically located at much lower redshift[14,15].

The line-free channels of the observations (Fig. 1) were used to constrain the underlying continuum emission. Our accurate position of the rest-frame 158 μm emission is indicated as a cross in Fig. 2 (right). We combine our continuum detections at 307 GHz and 112 GHz with published values and new Herschel Space Telescope observations to constrain the far-infrared properties of the source (see Supplementary Information for details). Our best fit gives a far-infrared luminosity of $L_{FIR} = (6.5 \pm 1) \times 10^{12} L_{Sun}$, a dust temperature of 35 ± 5 K (that is, broadly consistent with the average kinetic temperature of the molecular gas), a dust mass of $M_{dust} = (2.75 \pm 0.5) \times 10^8 M_{Sun}$ and a star formation rate of $850 M_{Sun}$ per year (with an uncertainty of about 30%). Given the extent of the source this results in an galaxy-averaged star formation rate surface density of $850 M_{Sun}$ per year divided by ($\pi(2.8$ kpc)^2) equalling $35 M_{Sun}$ per year kpc^{-2} (uncertainty ~50%), more than an order of magnitude less than found in nearby merging systems and a compact quasar host galaxy at $z = 6.42$ that has been studied in similar detail[10]. HDF 850.1 falls on the universal local star-formation law that relates the average surface density of the star formation rate to that of the molecular gas mass per local free-fall time[16]. The estimated surface density would increase if future observations resolved the source structure.

The resulting [C II]/far-infrared luminosity ratio of $L_{[C II]}/L_{FIR} = (1.7 \pm 0.5) \times 10^{-3}$ in HDF 850.1 is comparable to what is found in normal local star-forming galaxies[17], but is an order of magnitude higher than what is found in a $z = 6.42$ quasar[10], the only other high-z system where the [C II] emission could be resolved to date. Recent studies indicate that this ratio is a function of environment, with a low value ($L_{[C II]}/L_{FIR} \approx 1 \times 10^{-4}$) for luminous systems dominated by a central black hole (quasars) and a high ratio (up to $L_{[C II]}/L_{FIR} \approx 1 \times 10^{-2}$) for low-metallicity environments. Our relatively high ratio in $L_{[C II]}/L_{FIR}$ is consistent with HDF 850.1 being a high redshift star-forming system in a non-quasar environment[17].
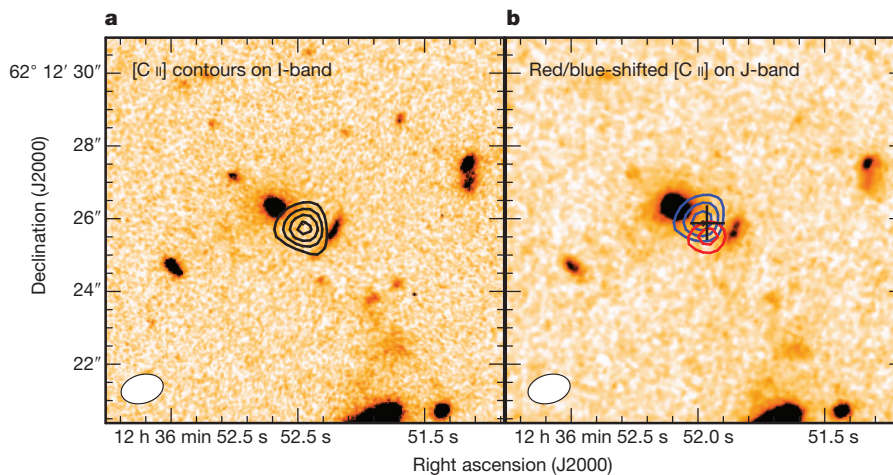

Figure 2 | [C II] line emission towards HDF 850.1. a, [C II] contours on top of a deep Hubble Space Telescope image[1] of the region in a filter (I band) that covers the Lyman-α line and ultraviolet continuum at $z = 5.183$. [C II] contours show the averaged emission over 700 km s^{-1} and are plotted at 5 mJy per beam, 7 mJy per beam, 9 mJy per beam and 11 mJy per beam ($1\sigma = 1.3$ mJy per beam). A Gaussian fit to the emission gives a deconvolved size of $0.9 \pm 0.3''$ or 5.7 ± 1.9 kpc at $z = 5.183$. The underlying continuum emission (not shown) is also extended on the same scales. **b**, The blue and red contours indicate the approaching and receding [C II] emission relative to the systemic redshift of $z = 5.183$. The colour shows a deep Hubble Space Telescope image in a longer wavelength filter (the J band from the Hubble Space Telescope's near-infrared camera and multi-object spectrometer (NICMOS))[29]. The cross indicates the position (and its 5σ uncertainty) of the rest-frame 158-μm continuum emission peak (right ascension 12 h 36 min 51.976 s, declination $62° 12' 25.80''$ in the J2000.0 system), consistent with earlier millimetre interferometric measurements[3,6] at lower resolution. The [C II] contours have been derived by averaging the spectrum (Fig. 1) from -400 km s^{-1} to 0 km s^{-1} and 0 km s^{-1} to $+400$ km s^{-1} and are plotted at levels of 7 mJy per beam, 10 mJy per beam and 13 mJy per beam ($1\sigma = 1.8$ mJy per beam), respectively. In each panel the beam size of the [C II] observations ($1.23'' \times 0.81''$) is indicated in the bottom left corner. From the spatial offset (total offset $= 0.9''$, that is, radius r is $0.45''$ or 2.8 kpc) and the FWHM of the line, we derive an approximate dynamical mass of $M_{dyn} \approx 3.4 \times 10^{10} M_{Sun}/(\sin i)^2$ where i is the (unknown) inclination of the system (using $M_{dyn}\sin^2 i = 1.3 \times (\text{FWHM}/2)^2 r/G$, where G is the gravitational constant[30]). These deep Hubble Space Telescope images of the Hubble Deep Field fail to reveal the (rest-frame) ultraviolet/optical counterpart of the galaxy that is forming stars at a rate of about $850 M_{Sun}$ per year.
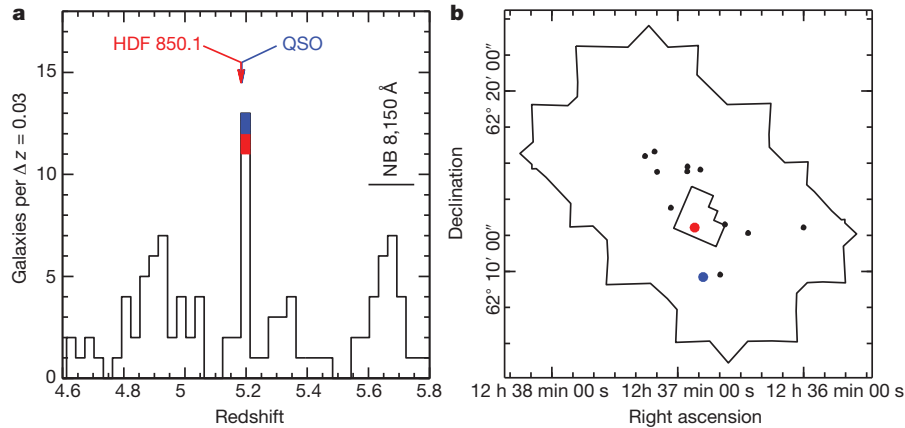
Figure 3 | Distribution of galaxies near HDF 850.1. a, Distribution of spectroscopic redshifts towards the Hubble Deep Field and its surroundings (from the Great Observatories Origins Deep Survey-North, GOODS-N). HDF 850.1 is indicated in red, and the quasar at the same redshift[18] is indicated in blue. There is an overdensity of galaxies in the redshift bin that contains HDF 850.1. The high source density at $z \approx 5.7$ is an observational artefact due to narrow-band Lyman-α imaging surveys of the region (with spectroscopic follow-up) that are sensitive to this particular narrow redshift range. **b**, Spatial coverage of the sources in the redshift bin $z = 5.183–5.213$. The small border indicates the size of the Hubble Deep Field; the larger border shows the surrounding area of GOODS-N. The presence of a strongly star-forming galaxy (HDF 850.1) and a quasar[18] in this region provides evidence for cosmic structure formation in the first billion years of the Universe. See Supplementary Information for more details.

An inspection of the distribution of galaxies towards HDF 850.1 that have spectroscopic redshifts shows that there is an overdensity of galaxies at the exact redshift of HDF 850.1, including a quasar at $z = 5.186$[18] (Fig. 3 and Supplementary Information). This makes this region one of the most distant galaxy overdensities known to date[19]. An elliptical galaxy at $z = 1.224$ (ref. 20) that is situated close to HDF 850.1 in projection (around $1''$ to the northeast) could potentially act as a gravitational lens for this source[3,4,21]. Using a velocity dispersion of $146\ \mathrm{km\ s^{-1}}$ in a singular isothermal sphere for this elliptical galaxy[4] and our new redshift and position of HDF 850.1, we derive an amplification factor of around 1.4. A similar flux amplification is found for a simple point source lens model with mass $3.5 \times 10^{11} M_{\mathrm{Sun}}$. This implies that even if lensing is occurring, the quantities derived here would not need to be revised significantly.

HDF 850.1 remains outstanding in the study of dust-obscured starbursts at high redshift, being one of the first such sources discovered, and yet evading detection in the optical and near-infrared. Its redshift of $z = 5.183$ enforces the presence of a high redshift tail ($z > 4$) of submillimetre bright star-forming galaxies (that is, a galaxy without an active galactic nucleus); currently there are only about half a dozen systems known[22–26]. Only a small fraction of submillimetre-bright sources is expected to be at very high redshift[27]—it is thus ironic that the first blank-field source belongs to this subgroup. HDF 850.1's large spatial extent, in combination with the modest CO excitation, the moderate surface density of its star-formation rate, and a high [C II]/far-infrared luminosity ratio, points to the presence of a spatially extended major starburst that is completely obscured even in the deepest Hubble Space Telescope images available for the Hubble Deep Field. The absence of a possible counterpart in the available deep imaging, even though the star-forming interstellar medium is distributed over many square kiloparsecs, makes this source extreme[22–24]. Given its high molecular gas mass ($3.5 \times (\alpha/0.8) \times 10^{10} M_{\mathrm{Sun}}$) and star-formation rate ($850 M_{\mathrm{Sun}}$ per year), HDF 850.1 can build a significant stellar component as early as $z \approx 4$ (ref. 28; a few hundred million years from $z \approx 5$). Blind line searches through spectral scans at millimetre wavelengths, as performed here, thus play a fundamental role in unveiling the nature of star-forming galaxies that are completely obscured in the (restframe) optical and ultraviolet even if multiwavelength data at unparalleled depth are available.

1. Williams, R. E. *et al.* The Hubble Deep Field: observations, data reduction, and galaxy photometry. *Astron. J.* **112**, 1335–1389 (1996).
2. Hughes, D. H. *et al.* A submillimetre survey of the Hubble Deep Field: unveiling dust-enshrouded star formation in the Early Universe. *Nature* **394**, 241–247 (1998).
3. Downes, D. *et al.* Proposed identification of Hubble Deep Field submillimeter source HDF 850.1. *Astron. Astrophys.* **347**, 809–820 (1999).
4. Dunlop, J. S. *et al.* Discovery of the galaxy counterpart of HDF 850.1, the brightest submillimetre source in the Hubble Deep Field. *Mon. Not. R. Astron. Soc.* **350**, 769–784 (2004).
5. Wagg, J. *et al.* A broad-band spectroscopic search for CO line emission in HDF850.1: the brightest submillimetre object in the Hubble Deep Field-north. *Mon. Not. R. Astron. Soc.* **375**, 745–752 (2007).
6. Cowie, L. L., Barger, A. J., Wang, W.-H. & Williams, J. P. An accurate position for HDF 850.1: the brightest submillimeter source in the Hubble Deep Field-north. *Astrophys. J.* **697**, L122–L126 (2009).
7. Carilli, C. L. & Yun, M. S. The radio-to-submillimeter spectral index as a redshift indicator. *Astrophys. J.* **513**, L13–L16 (1999).
8. Richards, E. A. Radio Identification of Submillimeter Sources in the Hubble Deep Field. *Astrophys. J.* **513**, L9–L12 (1999).
9. Solomon, P. M. & Vanden Bout, P. A. Molecular Gas at High Redshift. *Annu. Rev. Astron. Astrophys.* **43**, 677–725 (2005).
10. Walter, F. *et al.* A kiloparsec-scale hyper-starburst in a quasar host less than 1 gigayear after the Big Bang. *Nature* **457**, 699–701 (2009).
11. Alexander, D. *et al.* The Chandra Deep Field North survey. XIII. 2 ms point-source catalogs. *Astron. J.* **126**, 539–574 (2003).
12. Loenen, A. F. *et al.* Excitation of the molecular gas in the nuclear region of M 82. *Astron. Astrophys.* **521**, L2 (2010).
13. Downes, D. & Solomon, P. M. Rotating nuclear rings and extreme starbursts in ultraluminous galaxies. *Astrophys. J.* **507**, 615–654 (1998).
14. Tacconi, L. *et al.* Submillimeter galaxies at z ~ 2: evidence for major mergers and constraints on lifetimes, IMF, and CO-H2 conversion factor. *Astrophys. J.* **680**, 246–262 (2008).
15. Ivison, R. *et al.* Tracing the molecular gas in distant submillimetre galaxies via CO(1–0) imaging with the Expanded Very Large Array. *Mon. Not. R. Astron. Soc.* **412**, 1913–1925 (2011).
16. Krumholz, M. R., Dekel, A. & McKee, C. F. A universal, local star formation law in galactic clouds, nearby galaxies, high-redshift disks, and starbursts. *Astrophys. J.* **745**, 69 (2012).
17. Stacey, G. J. *et al.* A 158 μm [C II] line survey of galaxies at z ~ 1–2: an indicator of star formation in the early Universe. *Astrophys. J.* **724**, 957–974 (2010).
18. Barger, A. J. *et al.* X-ray, optical, and infrared imaging and spectral properties of the 1Ms Chandra Deep Field North sources. *Astron. J.* **124**, 1839–1885 (2002).
19. Capak, P. *et al.* A massive protocluster of galaxies at a redshift of z ≈ 5.3. *Nature* **470**, 233–235 (2011).
20. Barger, A. J., Cowie, L. L. & Wang, W.-H. A highly complete spectroscopic survey of the GOODS-N field. *Astrophys. J.* **689**, 687–708 (2008).
21. Hogg, D. W., Blandford, R., Kundic, T., Fassnacht, C. D. & Malhotra, S. A candidate gravitational lens in the Hubble Deep Field. *Astrophys. J.* **467**, L73–L75 (1996).
22. Riechers, D. A. *et al.* A massive molecular gas reservoir in the z = 5.3 submillimeter galaxy AzTEC-3. *Astrophys. J.* **720**, L131–L136 (2010).
23. Daddi, E. *et al.* Two bright submillimeter galaxies in a z = 4.05 protocluster in Goods-North, and accurate radio-infrared photometric redshifts. *Astrophys. J.* **694**, 1517–1538 (2009).
24. Schinnerer, E. *et al.* Molecular gas in a submillimeter galaxy at z = 4.5: evidence for a major merger at 1 billion years after the Big Bang. *Astrophys. J.* **689**, L5–L8 (2008).
25. Combes, F. *et al.* A bright z = 5.2 lensed submillimeter galaxy in the field of Abell 773. HLSJ091828.6+514223. *Astron. Astrophys.* **538**, L4 (2012).

26. Cox, P. *et al.* Gas and dust in a submillimeter galaxy at z = 4.24 from the Herschel atlas. *Astrophys. J.* **740,** 63 (2011).
27. Ivison, R. *et al.* A robust sample of submillimetre galaxies: constraints on the prevalence of dusty, high-redshift starbursts. *Mon. Not. R. Astron. Soc.* **364,** 1025–1040 (2005).
28. Wiklind, T. *et al.* A population of massive and evolved galaxies at z>~5. *Astrophys. J.* **676,** 781–806 (2008).
29. Dickinson, M. *et al.* The unusual infrared object HDF-N J123656.3+621322. *Astrophys. J.* **531,** 624–634 (2000).
30. Daddi, E. *et al.* Very high gas fractions and extended gas reservoirs in z = 1.5 disk galaxies. *Astrophys. J.* **713,** 686–707 (2010).

Supplementary Information is linked to the online version of the paper at www.nature.com/nature.

Author Contributions F.W. had the overall lead of the project. The Plateau de Bure Interferometer data were analysed by R.D., F.W., P.C., R.N., M.K. and D.D. The Jansky Very Large Array data reduction was performed by C.C., J.H. and L.L. The molecular gas excitation was led by A.W. Spectroscopic redshift information was provided by M.D., R.E., H.S., D.S. and D.P.S. The spectral energy distribution analysis, including new Herschel data, was led by E.D.C, D.E. and E.D. An updated lensing model was provided by D.D. All authors helped with the proposal, data analysis and interpretation.

Author Information Reprints and permissions information is available at www.nature.com/reprints. The authors declare no competing financial interests. Readers are welcome to comment on the online version of this article at www.nature.com/nature. Correspondence and requests for materials should be addressed to F.W. (walter@mpia.de).